References and Notes

1. Intergovernmental Panel on Climate Change, *Climate Change 2001: The Scientific Basis. Contribution of Working Group I to the Third Assessment Report of the IPCC*, J. T. Houghton *et al*., Eds. (Cambridge Univ. Press, Cambridge, 2001).
2. C. Vörösmarty *et al.*, *Eos* **83**, 241 (2002).
3. S. Manabe, R. J. Stouffer, *J. Clim.* **7**, 5 (1994).
4. S. Rahmstorf, A. Ganopolski, *Clim. Change* **43**, 353 (1999).
5. S. Rahmstorf, *Nature* **378**, 145 (1995).
6. W. S. Broecker, *Science* **278**, 1582 (1997).
7. R. B. Lammers, A. I. Shiklomanov, C. J. Vörösmarty, B. J. Peterson, *J. Geophys. Res.* **106**, 3321 (2001).
8. The Russian Federal Service for Hydrometeorology and Environment Monitoring (Roshydromet) monitors the discharge of Russian arctic rivers. We have compiled and digitized this database, which is available on our Web site (www.r-arcticnet.sr.unh.edu/) and from the National Snow and Ice Data Center (http://nsidc.org). The downstream stations from which the data in this paper come have been monitored almost continuously from 1936 to 1999, despite a general decline in the arctic hydrologic monitoring network that began in the mid 1980s (*29*). Roshydromet considers these stations to be of primary importance because of their proximity to the ocean. Stage height readings to the nearest centimeter were made daily, and cross-channel measurements of discharge for rating curve calibrations were made 25 to 30 times per year in each river. With these frequent calibrations, estimates of daily discharge from the rating curves were accurate to ±5%.
9. I. P. Semiletov *et al.*, in *The Freshwater Budget of the Arctic Ocean*, E. L. Lewis, Ed. (Kluwer Academic, Dordrecht, Netherlands, 2000), pp. 323–366.
10. I. A. Shiklomanov, A. I. Shiklomanov, R. B. Lammers, B. J. Peterson, C. J. Vörösmarty, in *The Freshwater Budget of the Arctic Ocean*, E. L. Lewis, Ed. (Kluwer Academic, Dordrecht, Netherlands, 2000), pp. 281–296.
11. N. I. Savelieva, I. P. Semiletov, L. N. Vasilevskaya, S. P. Pugach, *Prog. Oceanogr.* **47**, 279 (2000).
12. T. D. Prowse, P. O. Flegg, *Hydrol. Processes* **14**, 3185 (2000).
13. The statistical strength of the temporal trend in combined river discharge from the Eurasian arctic is greater than for individual rivers, because the estimated slope for the sum increases with the number of rivers but the standard error of this estimate increases only with the square root of the number of rivers. This leads to a more powerful test of the null hypothesis of no trend.
14. M. C. Serreze *et al.*, *Clim. Change* **46**, 159 (2000).
15. R. R. Dickson *et al.*, *J. Clim.* **13**, 2671 (2000).
16. R. E. Moritz, C. M. Bitz, E. J. Steig, *Science* **297**, 1497 (2002).
17. Global temperature changes were calculated using data from the NASA Goddard Institute for Space Studies (www.giss.nasa.gov/data/update/gistemp/), and temperature changes for the pan-arctic and Eurasian arctic were calculated using the database of New *et al.* (*30*).
18. B. Nijssen, G. M. O'Donnell, A. F. Hamlet, D. P. Lettenmaier, *Clim. Change* **50**, 143 (2001).
19. J. R. Miller, G. L. Russell, *Geophys. Res. Lett.* **27**, 1183 (2000).
20. M. Stieglitz, A. Giblin, J. Hobbie, M. Williams, G. Kling, *Global Biogeochem. Cycles* **14**, 1123 (2000).
21. HSP is defined in (*4*). In addition to river runoff, the Atlantic HSP includes meltwater from sea and continental ice and precipitation minus evaporation ($P - E$) over the ocean. The difference between basing hydrologic sensitivity on global or hemispheric temperature is small, because in greenhouse gas–induced warming, both hemispheres warm by similar amounts. When linking hydrologic changes to local temperature, such as for Greenland, one needs to take into account that local warming over Greenland could be twice the global mean; a ~10% accumulation increase per °C of local warming over Greenland, as found in Greeland Ice Core Project and Greenland Ice Sheet Project 2 ice core data, is then consistent with the slope shown in Fig. 4.
22. J. R. Miller, G. L. Russell, *J. Geophys. Res.* **97**, 2757 (1992).
23. S. Van Blarcum, J. R. Miller, G. L. Russell, *Clim. Change* **30**, 7 (1995).
24. It is difficult to discern long-term trends for major North American arctic rivers, because discharge records from downstream gauging stations are relatively short (~25 to 35 years). Regression analyses of Mackenzie (at Arctic Red) and Yukon (at Pilot Station) discharge records produces slopes of +0.6 km^3/year and −0.1 km^3/year for the two rivers, respectively, but neither is a statistically significant result. However, temperature trends over North America that are similar to Eurasian trends over the past century support potential arctic-wide increases in river discharge (*30*).
25. Modeling studies predict substantial increases in freshwater contributions from the Greenland ice sheet (*31*, *32*). Although arctic glaciers and sea ice are much smaller in volume than the Greenland ice sheet, additional freshwater could be derived from their meltdown (*33*, *34*). Finally, $P - E$ over the Arctic Ocean appears to have increased over the past century and is expected to continue to increase in the future (*19*).
26. S. Rahmstorf, *Clim. Dyn.* **12**, 799 (1996).
27. P. U. Clark, N. G. Pisias, T. F. Stocker, A. J. Weaver, *Nature* **415**, 863 (2002).
28. S. Rahmstorf, *Nature* **419**, 207 (2002).
29. A. I. Shiklomanov, R. B. Lammers, C. J. Vörösmarty, *Eos* **83**, 13 (2002).
30. M. New, M. Hulme, P. Jones, *J. Clim.* **13**, 2217 (2000).
31. P. Huybrechts, J. DeWolde, *J. Clim.* **12**, 2169 (1999).
32. M. Wild, A. Ohmura, *Ann. Glaciol.* **30**, 197 (2000).
33. J. A. Dowdeswell *et al.*, *Quat. Res.* **48**, 1 (1997).
34. K. Y. Vinnikov *et al.*, *Science* **286**, 1934 (1999).

35. We gratefully acknowledge the efforts of the personnel of the Russian Federal Service for Hydrometeorology and Environment Monitoring. We thank A. Solow of the Woods Hole Oceanographic Institute for thoughtful comments and advice on statistical analyses and R. Alley, I. Belkin, T. Stocker, D. Schindler, M. Stieglitz, and G. Holloway for their insights and advice. Supported by the Arctic System Science Program of NSF (grants NSF-OPP-9524740, NSF-OPP-9818199, and NSF-OPP-0229302) and NASA (NASA EOS grant NAG5-6137).

Supporting Online Material

www.sciencemag.org/cgi/content/full/298/5601/2171/DC1

Fig. S1

16 August 2002; accepted 7 November 2002

Soil Warming and Carbon-Cycle Feedbacks to the Climate System

J. M. Melillo,[1]* P. A. Steudler,[1] J. D. Aber,[2] K. Newkirk,[1] H. Lux,[1] F. P. Bowles,[3] C. Catricala,[1] A. Magill,[2] T. Ahrens,[1] S. Morrisseau[1]

In a decade-long soil warming experiment in a mid-latitude hardwood forest, we documented changes in soil carbon and nitrogen cycling in order to investigate the consequences of these changes for the climate system. Here we show that whereas soil warming accelerates soil organic matter decay and carbon dioxide fluxes to the atmosphere, this response is small and short-lived for a mid-latitude forest, because of the limited size of the labile soil carbon pool. We also show that warming increases the availability of mineral nitrogen to plants. Because plant growth in many mid-latitude forests is nitrogen-limited, warming has the potential to indirectly stimulate enough carbon storage in plants to at least compensate for the carbon losses from soils. Our results challenge assumptions made in some climate models that lead to projections of large long-term releases of soil carbon in response to warming of forest ecosystems.

The acceleration of global warming due to terrestrial carbon-cycle feedbacks may be an important component of future climate change (*1*). Recent experiments with fully coupled, three-dimensional carbon-climate models suggest that carbon-cycle feedbacks could substantially accelerate (*2*) or slow (*3*) climate change over the 21st century. Both the sign and magnitude of these feedbacks in the real Earth system are still highly uncertain because of gaps in basic understanding of terrestrial ecosystem processes (*2*, *3*). For example, the potential switch of the terrestrial biosphere from its current role as a carbon sink (*4*, *5*) to a carbon source is critically dependent upon the long-term sensitivity to global warming of the respiration of soil microbes, which is still a subject of debate (*6*–*8*). Here we present results from a long-term (10-year) soil warming experiment designed to explore this feedback issue in an ecosystem context.

We began our soil warming study in April 1991, in an even-aged mixed hardwood forest stand at the Harvard Forest in central Massachusetts (42.54°N, 72.18°W). Dominant tree

[1]The Ecosystems Center, Marine Biological Laboratory, Woods Hole, MA 02543, USA. [2]Complex Systems Research Center, University of New Hampshire, Durham, NH 03824, USA. [3]Research Designs, Post Office Box 26, Woods Hole, MA 02543, USA.

*To whom correspondence should be addressed. E-mail: jmelillo@mbl.edu

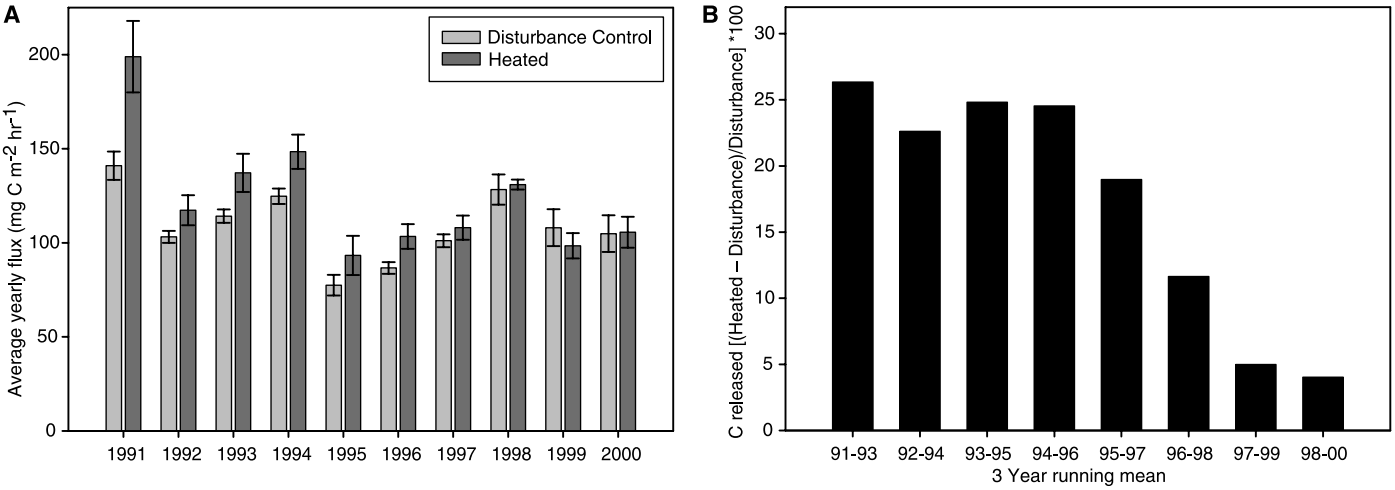

Fig. 1. (**A**) Average yearly fluxes of CO_2 from the heated and disturbance control plots. Measurements were made from April through November for the period from 1991 through 2000. Error bars represent the standard error of the mean (n = 6 plots) between plots of the same treatment. (**B**) Percentage increase in the amount of carbon released from the heated plots relative to the disturbance control plots. The data are presented as 3-year running means for the period from 1991 through 2000.

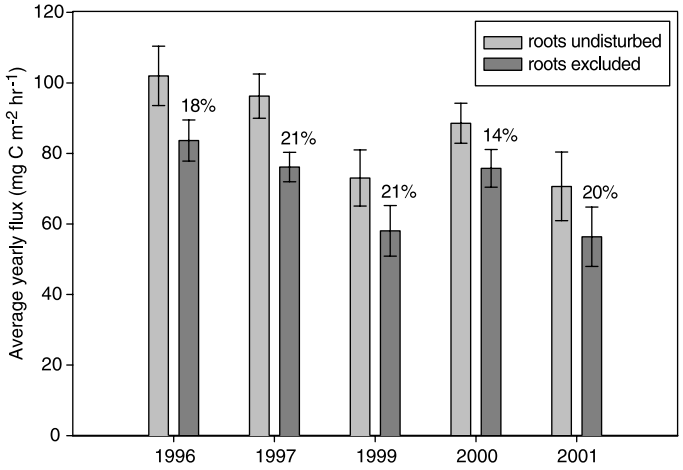

Fig. 2. Average yearly fluxes at the Harvard Forest trenched-plot experiment. Data represent average yearly CO_2 fluxes from unheated plots only, as measured by the static chamber technique. The trenched-plot experiment is a companion to the Harvard Forest soil warming experiment, in which we have used both trenching and heating to investigate the relative contributions of root and microbial respiration to total soil respiration under ambient and elevated temperature conditions. Methods of heating are the same as for the main soil warming experiment. Percentage values represent the contribution of roots to total soil respiration. Error bars represent the standard error of the mean (n = 3 plots) for each treatment. The same relative patterns were observed in the treatments that included heating and trenching.

species include paper birch (*Betula papyrifera* Marsh.), red maple (*Acer rubrum* L.), black oak (*Quercus velutina* Lam.), and striped maple (*Acer pennsylvanicum* L.). Soils are mainly of the Canton series (coarse-loamy over sandy or sandy-skeletal, mixed mesic Typic Dystrochrept), with a surface pH of 3.83 and a subsurface pH of 4.85. The average bulk density of the upper 15 cm is 0.64 g cm^{-3}. A distinct plow layer indicates past cultivation, and historical records confirm that this old-field forest was established after the abandonment of cultivation at the turn of the century. There has been some cutting for firewood after abandonment. The climate is cool temperate and humid. The mean weekly air temperature varies from a high of about 20°C in July to a low of about −6°C in January. Precipitation is distributed evenly throughout the year and annually averages about 108 cm.

The field manipulation contains 18 6-m-by-6-m plots that are grouped into six blocks. The three plots within each block are randomly assigned to one of three treatments. The treatments are (i) heated plots in which the average soil temperature is elevated 5°C above ambient by the use of buried heating cables, (ii) disturbance control plots that are identical to the heated plots except that they receive no electrical power, and (iii) undisturbed control plots that have been left in their natural state. In the heated and disturbance control plots, we buried heating cables at 10-cm depths spaced 20 cm apart. When supplied with 240 V of ac, the heating cables have a power output of 13.6 W m^{-2} and produce a power density of about 77 W m^{-2}. Heating cables are controlled by a data logger that monitors 42 thermistors (five in each heated plot and one in each undisturbed and disturbance control plot) every 10 min. Plots are turned on and off automatically to maintain a 5°C temperature differential between heated and control plots. This heating method works well under a variety of moisture and temperature conditions (*9*, *10*). We compared carbon and nitrogen dynamics measured in heated plots to those measured in disturbance control plots, to isolate heating effects from the effects of cable installation (such as root cutting and soil compaction).

We measured the (CO_2) evolution rates from the plots at least monthly from April through November throughout the 10-year study (*11*). The increase in CO_2 flux due to warming averaged about 28% over the first 6 years of the study. Over the last 4 years of the study, the "stimulatory" effect of warming on soil respiration markedly decreased (Fig. 1A). The 3-year running means we calculated show, from 1998 through 2000, only about a 5% increase in soil respiration in the warmed versus disturbance control plots (Fig. 1B). By the 10th year of the study, soil respiration showed no significant response to warming.

To partition the two components of soil respiration—microbial respiration and root respiration—we carried out a second field experiment that involved trenched plots to exclude roots and a soil warming treatment, in a full-factorial design in which there were three plots per treatment. We estimate that root respiration is about 20% of the total soil respiration, with microbial respiration accounting for the remaining 80% (Fig. 2).

Combining the soil respiration data from the warming study with data from the partitioning study, we estimate that carbon loss stimulated by warming for the entire 10-year period was 944 g m^{-2}. This amounts to about 11.3% of the soil carbon found in the top 60 cm of the soil profile.

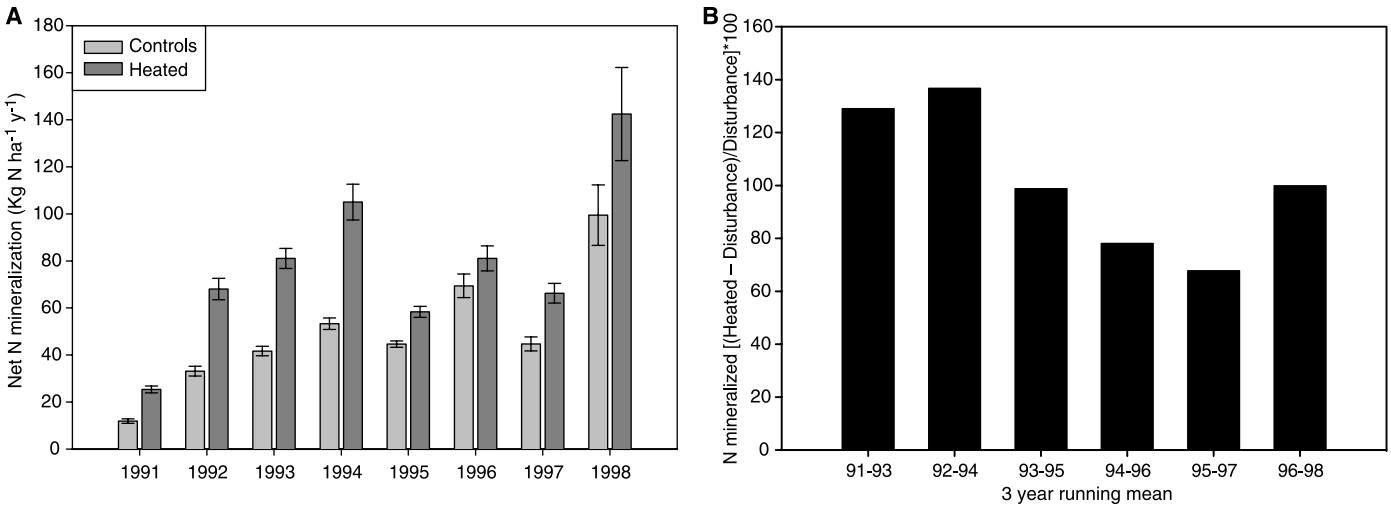

Fig. 3. (**A**) Average yearly net nitrogen mineralization rates measured in the heated and disturbance control plots at the Harvard Forest soil warming experiment. Measurements were made for the period from 1991 through 1998. Error bars represent the standard error of the mean (n = 6 plots) between plots of the same treatment. (**B**) Net nitrogen mineralization at the Harvard Forest soil warming experiment: percent increase in heated plots relative to the disturbance control plots. The data are presented as 3-year running means for the period from 1991 through 1998.

The relatively small and ephemeral loss of soil carbon we observed in response to a decade of warming is consistent with the prediction that these soils contain at least two pools of carbon that have different susceptibilities to microbial attack (*12*, *13*). One of these is composed of carbon compounds such as polysaccharides that are readily used by microorganisms as energy sources, and the other is made up of carbon compounds such as those with aromatic ring structures that are much more difficult for microbes to use. The decay rate of the first pool is very temperature-sensitive, whereas the decay rate of the second pool is not.

Using standard methods, we also measured the rates of net nitrogen mineralization, nitrogen leaching, and gaseous nitrogen (nitrous oxide) loss (*14*). Soil warming increased net nitrogen mineralization (Fig. 3A) but had no effect on either gaseous nitrogen losses or leaching of inorganic and organic nitrogen (*15*). The increases in net nitrogen mineralization were largest in the early years of the study (Fig. 3B). We estimate that over the entire 10-year study period, warming resulted in a cumulative increase in net nitrogen mineralization of 41 g m^{-2}.

How does this increase in nitrogen mineralization affect the ecosystem's capacity to store carbon? We can begin to address this question by using the results of our long-term nitrogen fertilization study at the Harvard Forest. In that study, we have been adding almost 5 g of nitrogen m^{-2} $year^{-1}$ for more than a decade to a hardwood forest stand very similar to the one we used for the soil warming study (*16*). After 9 years, we estimated that 12.7% of the total amount of nitrogen fertilizer added (approximately 45 g of nitrogen m^{-2}) ended up in the woody tissue of the stand's trees. If we assume that 12.7% of the increased amount of nitrogen made available by warming ended up in woody tissue, we estimate that this would result in an additional 1560 g m^{-2} of carbon storage in the vegetation over the decade of warming (*17*). Despite the uncertainties in both our estimates of carbon gains in the vegetation and measurements of carbon losses from soil due to soil warming, we conclude that the estimated vegetation gains are at least as large as the measured soil losses (*18*).

There is some direct field evidence that soil warming enhances carbon storage in trees. One example comes from a soil warming study in a Norway spruce forest at Flakaliden in northern Sweden (64°N). Using a soil warming design based on our Harvard Forest study, Linder and colleagues (*19*, *20*) warmed large (10 m by 10 m) forest plots in a long-term study. After 5 years, they found that there was a significant (more than 50%) increase in stem-wood growth of the trees on the heated plots relative to the controls.

The carbon balance of forest ecosystems in a climate-changed world would, of course, depend on more than soil warming. Carbon storage in woody tissue would also be affected by other factors related to climate change, including the availability of water, the effects of increased temperature on both plant photosynthesis and aboveground plant respiration, and the atmospheric concentration of CO_2. Reductions in soil moisture and increased plant respiration associated with warming will tend to reduce carbon storage in mid-latitude forests, whereas moderate increases in soil moisture and increased concentrations of CO_2 will likely increase carbon storage in these systems, especially if nitrogen limitation is relieved.

Warming experiments in mid-latitude ecosystems without a dominant woody vegetation component, such as alpine meadows (*21*) and grasslands (*22*), have shown either small carbon losses or little change in carbon storage. Warming may have its largest positive feedback effects in high-latitude ecosystems that contain small-stature and/or sparse woody vegetation and large pools of partially decomposed soil carbon that have accumulated under cold, wet conditions. If these soils undergo both warming and drying, they have the potential to lose large amounts of carbon as CO_2 to the atmosphere (*13*).

The Harvard Forest warming study demonstrates the potential importance of understanding how microbial respiration in soils responds to global warming and how temperature-driven changes in the nitrogen cycle will affect the capacity of forest ecosystems to store carbon. The possibility that warming can lead to both positive and negative feedbacks to the climate system suggests that it is essential that we accurately represent them in coupled atmosphere-ocean-land general circulation models if we are to successfully predict climate change over the next decades.

References and Notes

1. G. M. Woodwell, F. T. MacKenzie, Eds., *Biotic Feedbacks in the Global Climatic System: Will the Warming Feed the Warming?* (Oxford Univ. Press, New York, 1995), pp. 3–21.
2. P. M. Cox, R. A. Betts, C. D. Jones, S. A. Spall, I. J. Totterdell, *Nature* **408**, 184 (2000).
3. P. Friedlingstein, J.-L. Dufresne, P. M. Cox, P. Rayner, *Tellus*, in press.
4. J. T. Houghton *et al.*, Eds., *Climate Change 2001: The Scientific Basis* (Cambridge Univ. Press, Cambridge, 2001).
5. D. S. Schimel *et al.*, *Nature* **414**, 169 (2001).
6. C. P. Giardina, M. G. Ryan, *Nature* **404**, 858 (2000).
7. Y. Luo, S. Wan. D. Hui, L. L. Wallace, *Nature* **413**, 622 (2001).

8. L. Rustad, *Nature* **413**, 578 (2001).
9. W. T. Peterjohn, J. M. Melillo, F. P. Bowles, P. A. Steudler, *Oecologia* **93**, 18 (1993).
10. W. T. Peterjohn, J. M. Melillo, P. A. Steudler, K. M. Newkirk, *Ecol. Appl.* **4**, 617 (1994).
11. CO_2 flux measurements were made by placing chamber lids over anchored collars for 15 min and sampling the headspace at 5-min intervals. Samples were analyzed for trace gas concentrations by gas chromatography or infrared analysis, and the changes in concentration were used to calculate net flux rates. On each sampling date, fluxes were measured at early morning and afternoon intervals.
12. J. Grace, M. Rayment, *Nature* **404**, 819 (2000).
13. E. A. Davidson, S. E. Trumbore, R. Amundson, *Nature* **408**, 789 (2000).
14. Net nitrogen mineralization was measured for the organic horizon and upper 10 cm of mineral soil using in situ buried bag incubations. Incubations were for 6 weeks at a time, from April through November, and for 4 months during the winter. Initial samples were collected and analyzed for extractable NH_4^+ and NO_3^- content (extraction with 2N KCl for 48 hours and analysis with standard autoanalyzer methods). The same analysis was carried out on the incubated samples. The difference in total mineral N content between initial and incubated soils is the net mineralization rate. Soil nitrogen was assessed through sampling of organic and mineral soils in all plots in 1992 and again in 1999. Samples were analyzed for carbon and nitrogen content with a Perkin-Elmer CHN analyzer. Concentrations of inorganic nitrogen in water leaching below the rooting zone were measured with high-tension lysimetry. Soil water samples were collected from one porous cup lysimeter per plot on two occasions every month for the first 2 years of the experiment, then once monthly. Lysimeters were placed at a depth of 50 cm and evacuated to 15 inches of mercury for 24 hours before sampling. Samples were frozen until they were analyzed for NH_4^+ and NO_3^-. Nitrous oxide fluxes were measured along with CO_2, with the same static chamber method, from 1991 through 1995. Samples were analyzed for trace gas concentrations by gas chromatography, and the changes in concentration were used to calculate net flux rates.
15. During 1996, we analyzed the lysimeter water samples for dissolved organic nitrogen (DON). We found very low levels of DON in lysimeters from all treatments with no clear treatment differences. DON was estimated as the difference between total dissolved nitrogen (TDN) and dissolved inorganic nitrogen, where TDN was measured by high-temperature platinum–catalyzed combustion (*23*).
16. A. H. Magill *et al*., *Ecosystems* **3**, 238 (2000).
17. This additional carbon storage in woody tissue was calculated as the product of 12.7% of the cumulative increase in net nitrogen mineralization over the decade (41 g of nitrogen m^{-2}) and the measured carbon:nitrogen mass ratio of the wood (300:1) as follows: 0.127×4 g of nitrogen $m^{-2} \times 300$.
18. This conclusion is based on a paired Student's *t* test with aggregated data from the six experimental blocks.
19. J. Bergh, S. Linder, T. Lundmark, B. Elfving, *For. Ecol. Manage.* **119**, 51 (1999).
20. P. Jarvis, S. Linder, *Nature* **405**, 904 (2000).
21. J. Harte *et al*. *Ecol. Appl.* **5**, 132 (1995).
22. Y. Luo, S. Wan, S. Hui, L. Wallace, *Nature* **413**, 622 (2001).
23. J. Merriam, W. H. McDowell, W. S. Currie, *Soil Sci. Soc. Am. J.* **60**, 1050 (1996).
24. Supported by the Office of Science, Biological and Environmental Research Program, U.S. Department of Energy, through the Northeast Regional Center of the National Institute for Global Environmental Change under cooperative agreement no. DE-FC03-90ER61010; NSF's Long-Term Ecological Research Program (contract no. NSF-DEB 0080592); the U.S. Environmental Protection Agency's Global Change Program (contract no. EPA-CR 823713-01-0); and the ExxonMobil Corporation.

20 May 2002; accepted 7 November 2002

Shape-Controlled Synthesis of Gold and Silver Nanoparticles

Yugang Sun and Younan Xia*

Monodisperse samples of silver nanocubes were synthesized in large quantities by reducing silver nitrate with ethylene glycol in the presence of poly(vinyl pyrrolidone) (PVP). These cubes were single crystals and were characterized by a slightly truncated shape bounded by {100}, {110}, and {111} facets. The presence of PVP and its molar ratio (in terms of repeating unit) relative to silver nitrate both played important roles in determining the geometric shape and size of the product. The silver cubes could serve as sacrificial templates to generate single-crystalline nanoboxes of gold: hollow polyhedra bounded by six {100} and eight {111} facets. Controlling the size, shape, and structure of metal nanoparticles is technologically important because of the strong correlation between these parameters and optical, electrical, and catalytic properties.

Metal nanoparticles play important roles in many different areas. For example, they can serve as a model system to experimentally probe the effects of quantum confinement on electronic, magnetic, and other related properties (*1*–*3*). They have also been widely exploited for use in photography (*4*), catalysis (*5*), biological labeling (*6*), photonics (*7*), optoelectronics (*8*), information storage (*9*), surface-enhanced Raman scattering (SERS) (*10*, *11*), and formulation of magnetic ferrofluids (*12*). The intrinsic properties of a metal nanoparticle are mainly determined by its size, shape, composition, crystallinity, and structure (solid versus hollow). In principle, one could control any one of these parameters to fine-tune the properties of this nanoparticle.

Department of Chemistry, University of Washington, Seattle, WA 98195–1700, USA.

*To whom correspondence should be addressed. E-mail: xia@chem.washington.edu

Many metals can now be processed into monodisperse nanoparticles with controllable composition and structure (*13*) and sometimes can be produced in large quantities through solution-phase methods (*14*, *15*). Despite this, the challenge of synthetically controlling the shape of metal nanoparticles has been met with limited success. On the nanometer scale, metals (most of them are face-centered cubic, or fcc) tend to nucleate and grow into twinned and multiply twinned particles (MTPs) with their surfaces bounded by the lowest-energy {111} facets (*16*). Other morphologies with less stable facets have only been kinetically achieved by adding chemical capping reagents to the synthetic systems (*17*–*22*). Here we describe a solution-phase route to the large-scale synthesis of silver nanocubes. Uniform gold nanoboxes with a truncated cubic shape were also generated by reacting the silver cubes with an aqueous $HAuCl_4$ solution.

The primary reaction involved the reduction of silver nitrate with ethylene glycol at 160°C. In this so-called polyol process (*23*), the ethylene glycol served as both reductant and solvent. We recently demonstrated that this reaction could yield bicrystalline silver nanowires in the presence of a capping reagent such as poly(vinyl pyrrolidone) (PVP) (*24*). Subsequent experiments suggested that the morphology of the product had a strong dependence on the reaction conditions. When the concentration of $AgNO_3$ was increased by a factor of 3 and the molar ratio between the repeating unit of PVP and $AgNO_3$ was kept at 1.5, single-crystalline nanocubes of silver were obtained (*25*). Figure 1, A and B, show scanning electron microscope (SEM) images of a typical sample of silver nanocubes and indicate the large quantity and good uniformity that were achieved using this approach. These silver nanocubes had a mean edge length of 175 nm, with a standard deviation of 13 nm. Their surfaces were smooth, and some of them self-assembled into ordered two-dimensional (2D) arrays on the silicon substrate when the SEM sample was prepared. It is also clear from Fig. 1B that all corners and edges of these nanocubes were slightly truncated. Figure 1C shows the transmission electron microscope (TEM) image of an array of silver nanocubes self-assembled on the surface of a TEM grid. The inset shows the electron diffraction pattern obtained by directing the electron beam perpendicular to one of the square faces of a cube. The square symmetry of this pattern indicates that each silver nanocube was a single crystal bounded mainly by {100} facets. On the basis of these SEM and TEM studies, it is clear that the slightly truncated nanocube could be described by the drawing shown in